FIRST OBSERVATION OF CONTROLLED BEAM-HALO POPULATION AND CLEANING AT THE LHC BY AN AC DIPOLE

D. Veres*, D. Butti, F. Capoani, J. Dilly, M. Giovannozzi, S. Kostoglou, B. Lindstrom, E. Maclean, D. Valuch, European Organization for Nuclear Research, Geneva, Switzerland
G. Franchetti, GSI Helmholtz Centre for Heavy Ion Research, Darmstadt, Germany

Abstract

Experimental observations indicate that a significant fraction of the stored beam energy in the CERN Large Hadron Collider (LHC) is contained in the transverse beam halo. Combined with the anticipated increase in beam brightness in the High-Luminosity LHC (HL-LHC) and new expected fast failure scenarios resulting in a loss of large-amplitude particles, an overpopulated beam halo poses risk to the safe operation of the machine. Following removal from the HL-LHC baseline of the Hollow Electron Lens, which was studied as the preferred method for active halo control, alternative halo-cleaning methods need to be investigated. A novel method being explored is the use of an AC multipole operated in resonance with the betatron tune to create a stable island in phase space in which halo particles are adiabatically trapped and transported to the collimators in a controlled manner. This paper presents the results of the first successful proof-of-principle measurement of both controlled beam-halo population and cleaning using an AC dipole at the LHC.

INTRODUCTION

Non-linear beam manipulations, including the CERN Proton Synchrotron Multi-Turn Extraction (MTE) [1–6], have emerged as promising means of novel beam manipulations. Recently, exciter devices have been considered [7] and have found promising applications, among others, as beam-halo cleaners [8].

In June 2025, an eight-hour proof-of-principle test of halo cleaning with stable islands at the LHC [9] was performed. The transverse feedback (ADT) was used for the custom AC dipolar excitation during the measurement. The study was carried out at the injection energy of 450 GeV, which allowed efficient re-injection of bunches when needed and scanning parameters. Ten low-intensity bunches with approximately 4.5×10^{10} protons per bunch were injected each time, with a normalised beam emittance of 2 µm in both planes, and only Beam 1 (clockwise beam) was used.

EXCITATION PROTOCOLS

Several excitation protocols were tested: the bunches were first blown up using the ADT to create different normalised emittance bunches in the 2 µm to 4.5 µm range; halo cleaning was applied directly after the bunches were injected relying on the natural population of the tails; the excitation was adapted to populate the tails first before cleaning. Finding the optimal excitation protocol took longer than expected, resulting in insufficient time to perform a chromaticity scan, and therefore measurements were only performed at $Q'_x = Q'_y = 3$.

Furthermore, measurements were hindered by the observation that despite the excellent correction of the linear coupling ($|c_-| = 0.001$), the excitation applied in the horizontal plane was strongly felt by the vertical plane as well, and vice versa, as evidenced by a very clear peak observed in the tune spectrum measured by the Band-Based Tune (BBQ) pickup. Hence, it was decided to proceed with only vertical excitations that left the horizontal plane undisturbed because of the lower fractional tune in the horizontal plane ($Q_x = 62.28$, $Q_y = 60.30$ at injection into the LHC).

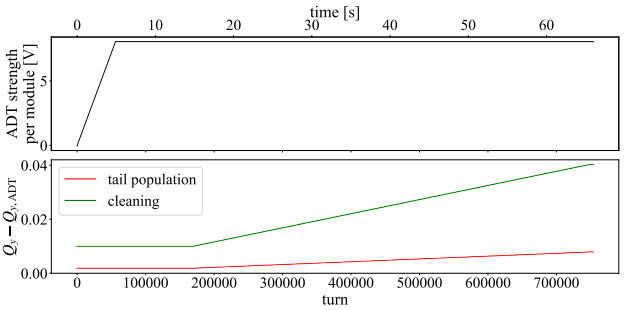

Figure 1: Excitation protocol used during the measurement.

Halo cleaning could be best observed when the tails were intentionally populated first. Hence, the same excitation protocol was applied as for cleaning, but the starting and end frequencies were adjusted to be much closer to the vertical tune. This resulted in the trapping of a significant number of particles in the beam core (approximately 15%) that were then displaced to larger amplitudes (still below that of the collimators) to form the halo. The excitation protocols applied during the population and the cleaning of the tail are shown in Fig. 1. To measure the tail population, a single excitation, as shown in Fig. 1, was sufficient, whereas effectively depleting the halo required applying this function at least five times in succession.

DATA ANALYSIS AND RESULTS

The transverse beam profile was recorded using both the Wire Scanners (WS) and the Beam Synchrotron Radiation Telescope (BSRT), which uses synchrotron light emitted by the protons. Due to the invasive nature of wire scans, they cannot be performed continuously, but the BSRT records and logs the beam profile approximately every second. However, the BSRT has a finite line-spread function that limits the resolution as well as the signal-to-noise ratio. Therefore,

* dora.erzsebet.veres@cern.ch

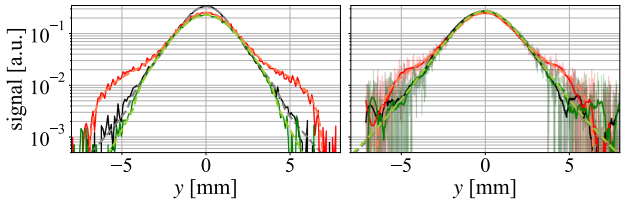

Figure 2: Vertical WS (left) and BSRT (right) profiles before (black) and after tail population (red) and after cleaning (green). For the BSRT profiles both the raw data (transparent) and the smoothed profiles (solid lines) are shown. Dashed lines in lighter shades show the fitted profiles.

during the measurement, wire scans were taken before and after each tail population and full cleaning to obtain an accurate representation of the beam profile, while the BSRT was used to continuously monitor the trends in the halo content.

Figure 2 shows profiles (without emittance blow-up) before and after the population of the tail and after 5 cleaning repetitions. The formation and reduction of heavy tails is apparent. Note that we consider particles to be in the halo if they are at large action (typically above 3σ, the limit may depend on the context) in either or both transverse planes. As it is impossible to perform tomography to accurately assess halo content, the Abel transform [10, 11] was used to recover beam profiles as a function of action under the reasonable assumption of circular symmetry of the 2D distribution and linear dynamics.

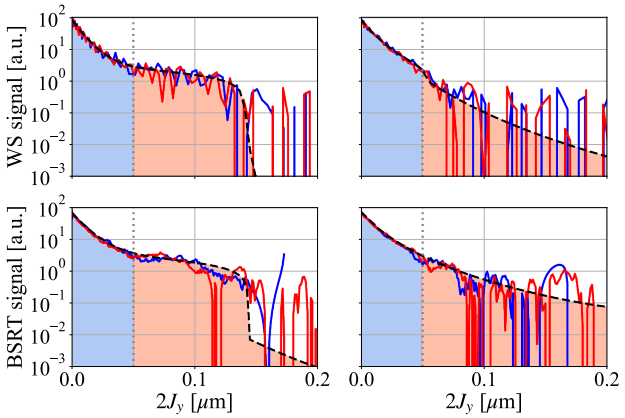

Figure 3: Vertical profiles as a function of action after tail population (left) and after cleaning (right). The blue and red lines show the left- and right-mirrored profiles, respectively, while the black dashed line shows the fitted profile.

Circular symmetry also implies that left-right y-projections are symmetric, and numerical implementations of the Abel transform [12] are sensitive to left-right asymmetry even at the level of noise in the measured profiles. Therefore, the halo content was extracted separately from three profiles: one constructed by mirroring the left side of the original profile; one constructed by mirroring the right side; and one that was fitted by the symmetric function

$$f(y) = w\frac{\sqrt{\beta_1}}{C(q)}e_q(-\beta_1 y^2) + (1-w)\frac{\sqrt{\beta_2}}{C(0)}e_0(-\beta_2 y^2)$$

$$e_q(x) = \begin{cases} e^x, & \text{if } \tilde{q} = 0, \\ [1+\tilde{q}x]^{1/\tilde{q}}, & \text{if } 1+\tilde{q}x \geq 0 \text{ and } \tilde{q} \neq 0, \\ 0, & \text{if } 1+\tilde{q}x < 0 \text{ and } \tilde{q} \neq 0 \end{cases} \tag{1}$$

with $\tilde{q} = 1 - q$ and

$$C(q) = \begin{cases} \dfrac{2\sqrt{\pi}\Gamma\left(\frac{1}{1-q}\right)}{(3-q)\sqrt{1-q}\Gamma\left(\frac{3-q}{2(1-q)}\right)}, & \text{if } q < 1, \\ \sqrt{\pi}, & \text{if } q = 1, \\ \dfrac{\sqrt{\pi}\Gamma\left(\frac{3-q}{2(q-1)}\right)}{\sqrt{q-1}\Gamma\left(\frac{1}{q-1}\right)}, & \text{if } 1 < q < 3, \end{cases} \tag{2}$$

and q, β_1, β_2, w are the fit parameters. This function was selected because it conveniently and accurately reproduces the fairly standard profiles obtained before the tail population and after cleaning, as well as the non-standard profiles generated by the tail population for the purpose of performing the Abel transform, and the two terms $f(y)$ do not possess any specific physical significance. BSRT profiles were first smoothed using a Saviczky-Golay filter [13] with a third-order polynomial and then the mirrored and fitted BSRT profiles were also numerically deconvolved with the Gaussian line-spread function. The fits of the original profiles are shown in Fig. 2 (dashed lines). Figure 3 shows profiles as a function of action after population of the tail and cleaning.

After cleaning, the profiles are generally well approximated by a q-Gaussian function, in which case the w parameter always approaches 1 and the q parameter corresponds to the q value of the distribution. In these cases, the β_2 obtained from the BSRT profile fits is somewhat unstable. However, the weight of the second term in $f(y)$ is negligible and thus the quality of the fit is not significantly degraded. Note that when the tails are populated, the q parameter counter-intuitively decreases, but in this case the distribution is no longer a q-Gaussian and the q parameter loses its meaning.

The halo and core content were calculated as the area under the radial profiles above and below a given action J_{lim} corresponding to the expected amplitude of the stable fixed point of the island at approximately 3.5σ of the measured profiles at the injection of the bunches (dotted grey line in Fig. 3). The final values were obtained as the average between the values corresponding to the left-mirrored, right-mirrored, and fitted curves. The evolution of the halo-to-core ratio and the fraction of intensity in the core and halo as a function of time along with the tune of the ADT excitation are shown in Fig. 4. The BSRT results are generally quite consistent with the WS measurements, except in the case of the low halo fractions, which the BSRT somewhat overestimates. This is a regime particularly sensitive to noise, and it is nevertheless visible that all three observables

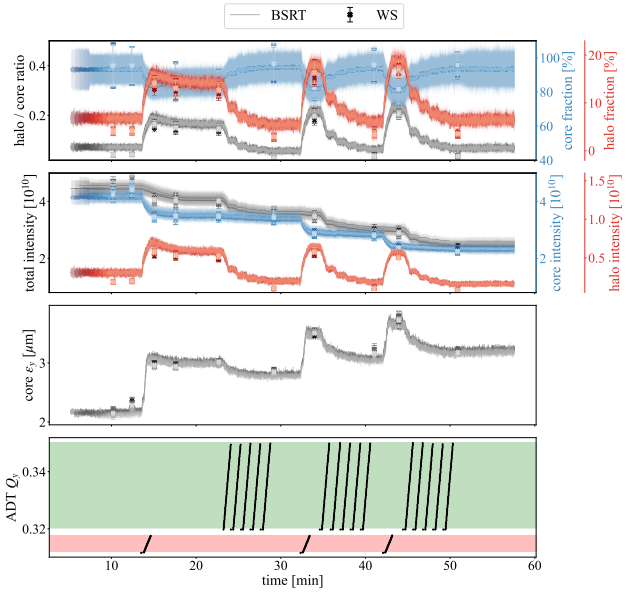

Figure 4: Halo-to-core ratio, fraction of intensity in core and halo (first plot), total intensity, in core and in halo (second plot), normalised Gaussian emittance of core (third plot) and tune of the ADT excitation (fourth plot) vs time during the manipulation. Excitation tunes resulting in tail population are shaded in red, those resulting in cleaning are shaded in green. Different shades in the top plots correspond to different bunches.

evolve in agreement with the applied excitation. During the tail population, there is a sharp increase in the halo content, while there is a steady decrease during the repeated application of the cleaning. WS measurements show that the ratio halo-to-core was reduced to 0.031 after the first cleaning from the initial value of 0.044, which corresponds to a 30% decrease.

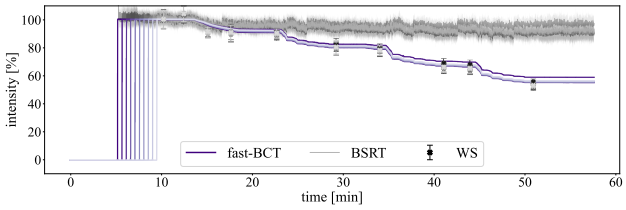

Figure 5: Intensity evolution from area under WS and BSRT profiles compared to the intensity reported by the fast-BCT. Different shades correspond to different bunches.

However, it is important to assess whether the tail population and cleaning result in any significant disturbance to the core, in particular unwanted core losses or blow-up. For this, the core and halo intensities must be calculated. Since the WS gain was not adjusted during the measurement, the evolution of the area under the WS profile curves was consistent with the intensity evolution reported by the bunch-by-bunch beam current transformer (FBCT). However, the same was not true for the BSRT data, as shown in Fig. 5, due to an automatic gain adjustment in the BSRT that aims to maintain the signal reaching the camera at a constant level regardless of the beam intensity. The injected intensities of each bunch could be used to calibrate the halo and core content from the first WS profiles, which could then be propagated to recover the halo and core intensities throughout the measurement. The halo and core intensities reported by the BSRT were calculated by calibrating the areas with the intensities reported by the FBCT.

The results are shown in Fig. 4 (second plot) along with the normalised core emittance obtained by fitting the profiles below J_{lim} with a Gaussian (third plot). WS measurements indicate that the first, second, and third cleaning resulted in approximately 1.72% (78.0%), 2.08% (80.7%) and 4.62% (84.0%) core (halo) intensity loss, respectively, indicating a very efficient halo cleaning with almost negligible core losses. However, the first, second, and third tail population resulted in approximately 13.95%, 4.13% and 2.35% total intensity loss, while this excitation was expected to be lossless. It should be noted that during the first tail population, the exciter was kept on for several minutes at the final frequency. This resulted in significantly more intensity loss than in the other two cases, but the source of this effect was not understood and requires further study. Additional studies would be beneficial to try to reduce the losses observed during the last two iterations of the tail population even further. Finally, Fig. 4 (third plot) shows that while cleaning is very efficient in reducing the halo content even below the values after injection, the core emittance increases with respect to the injected value, qualitatively in agreement with the expectations from simulations [9], although the magnitude may be enhanced by intrabeam scattering (IBS) effects, not considered in simulations.

CONCLUSIONS AND OUTLOOK

The results of the first proof-of-principle test of a new halo-cleaning method using a stable island generated by an AC dipole exciter were presented. Beam profile measurements, obtained using WS and BSRT, consistently confirmed both the intentional halo population and the cleaning using a specific ADT excitation. The observations of the cleaning were consistent with expectations: an AC dipole can be used to efficiently remove the halo with some unavoidable but mostly small core losses and core blow-up.

The dependence on (large) chromaticity was not tested because of the lack of time, and excitation was not possible in the horizontal plane because of an unexplained large coupling resulting in vertical blow-up.

The interplay between the exciter and other diffusion-inducing effects in a real accelerator, such as IBS should also be investigated. For an operational implementation of the cleaning protocol, measurements and demonstration of the feasibility at top energy are crucial.

ACKNOWLEDGEMENTS

The authors express their gratitude to the LHC Operations crew for support during the experimental investigations.

REFERENCES

[1] R. Cappi and M. Giovannozzi, "Novel method for multiturn extraction: trapping charged particles in islands of phase space", *Phys. Rev. Lett.*, vol. 88, no. 10, p. 104801, 2002. doi:10.1103/PhysRevLett.88.104801

[2] R. Cappi and M. Giovannozzi, "Multiturn extraction and injection by means of adiabatic capture in stable islands of phase space", *Phys. Rev. Spec. Top. Accel. Beams*, vol. 7, no. 2, p. 024001, 2004. doi:10.1103/PhysRevSTAB.7.024001

[3] J. Borburgh *et al.*, "First implementation of transversely split proton beams in the CERN Proton Synchrotron for the fixed-target physics programme", *Europhys. Lett.*, vol. 113, no. 3, 34001. 6 p, 2016. doi:10.1209/0295-5075/113/34001

[4] A. Huschauer *et al.*, "Transverse beam splitting made operational: Key features of the multiturn extraction at the CERN Proton Synchrotron", *Phys. Rev. Accel. Beams*, vol. 20, no. 6, p. 061001, 2017. doi:10.1103/PhysRevAccelBeams.20.061001

[5] M. Vadai, A. Alomainy, H. Damerau, M. Giovannozzi, and A. Huschauer, "Barrier bucket gymnastics and transversely split proton beams: Performance at the CERN Proton and Super Proton Synchrotrons", *Phys. Rev. Accel. Beams*, vol. 25, no. 5, p. 050101, May 2022. doi:10.1103/PhysRevAccelBeams.25.050101

[6] A. Huschauer *et al.*, "Advancing the CERN Proton Synchrotron multiturn extraction towards the high-intensity proton beams frontier", *Phys. Rev. Accel. Beams*, vol. 22, no. 10, p. 104002, Oct. 2019. doi:10.1103/PhysRevAccelBeams.22.104002

[7] A. Bazzani, F. Capoani, and M. Giovannozzi, "Analysis of adiabatic trapping phenomena for quasi-integrable area-preserving maps in the presence of time-dependent exciters", *Phys. Rev. E*, vol. 106, no. 3, p. 034204, Sep. 2022. doi:10.1103/PhysRevE.106.034204

[8] F. Capoani, A. Bazzani, and M. Giovannozzi, "Cleaning the beam halo using nonlinear ac magnets", *Phys. Rev. Accel. Beams*, vol. 28, no. 1, p. 014001, Jan. 2025. doi:10.1103/PhysRevAccelBeams.28.014001

[9] D. E. Veres, "Non-linear manipulations of charged particle beams with bent crystals and transverse exciters", PhD Dissertation, Goethe University, Germany, 2026.

[10] N. H. Abel, "Untersuchungen über die Reihe $1 + \frac{m(m-1)}{1\cdot 2}x + \frac{m(m-1)(m-2)(m-3)}{1\cdot 2\cdot 3\cdot 4}x^2 + \ldots$", *Journal für die reine und angewandte Mathematik*, vol. 1, pp. 311–339, 1826.

[11] RN. Bracewell, *The Fourier Transform and Its Applications*. McGraw-Hill, 1986. https://books.google.ch/books?id=Bk_vAAAAMAAJ

[12] D. D. Hickstein, S. T. Gibson, R. Yurchak, D. D. Das, and M. Ryazanov, "A direct comparison of high-speed methods for the numerical Abel transform", *Review of Scientific Instruments*, vol. 90, no. 6, p. 065115, 2019. doi:10.1063/1.5092635

[13] A. Savitzky and M. J. E. Golay, "Smoothing and differentiation of data by simplified least squares procedures", *Analytical Chemistry*, vol. 36, no. 8, pp. 1627–1639, 1964. doi:10.1021/ac60214a047